Leaf trichomes reduce boundary layer conductance

Thomas Buckley[1], Marshall A. Pierce[1], and Lawren Sack[2]

[1]University of California Davis Department of Plant Sciences
[2]UCLA Department of Ecology and Evolutionary Biology

January 18, 2022

Abstract

Leaf trichomes (hairs) have multiple hypothesized functions, of which several require empirical evidence. An important, yet controversial, proposed function of trichomes is to influence the leaf boundary layer, which would affect leaf temperature, transpiration and photosynthesis, and may confer differential benefits depending on climate. We used dynamic infrared thermography to test whether trichomes reduce the boundary layer conductance to heat (g_{bh}), impeding heat transfer between leaves and air. For five species, with trichome lengths of 135-780 μm, we transiently heated leaves with a radiative light source, measured the time constant for subsequent leaf cooling simultaneously in two adjacent leaf regions (with and without trichomes) with an IR camera, and inferred g_{bh} using an energy balance model. Cooling was slower in hairy leaf regions relative to bald regions, corresponding to a lower g_{bh} in hairy regions, by 2.4% to 39% across species. Contrary to prior theory, the resistance added by trichomes was unrelated to the depth of the hair layer (i.e., trichome height) across species. Simulations predicted that the reduction in g_{bh} by trichomes would influence energy balance and gas exchange rates by up to a few percent, with the direction and magnitude of such effects depending sensitively on environmental conditions.

Leaf trichomes reduce boundary layer conductance

Marshall A. Pierce[1], Lawren Sack[2], Thomas N. Buckley[1*]

1 Department of Plant Sciences, University of California, Davis, Davis, CA 95616

2 Department of Ecology and Evolutionary Biology, University of California, Los Angeles, Los Angeles, CA

* Author for correspondence: tnbuckley@ucdavis.edu, 530-752-0320

ORCID : Thomas N. Buckley: 0000-0001-7610-7136, Lawren Sack: 0000-0002-7009-7202

Summary statement : We provide the first unambiguous experimental proof that leaf trichomes (colloquially known as leaf hairs) slow down the transport of heat between leaves and the air.

Short title : Leaf trichomes reduce boundary layer conductance

Author contributions : TNB and LS conceived the project. TNB and MAP refined the project scope, designed and built the apparatus, and conducted the experiments. TNB performed the analysis and modeling. MAP and TNB drafted the manuscript. All authors edited the manuscript.

Funding information : This work was supported by the National Science Foundation (Award #1951244) and the USDA National Institute of Food and Agriculture (Hatch Project 1016439).

Keywords : trichomes, leaf hairs, boundary layer conductance, boundary layer resistance

Abstract

Leaf trichomes (hairs) have multiple hypothesized functions, of which several require empirical evidence. An important, yet controversial, proposed function of trichomes is to influence the leaf boundary layer, which would affect leaf temperature, transpiration and photosynthesis, and may confer differential benefits depending on climate. We used dynamic infrared thermography to test whether trichomes reduce the boundary layer conductance to heat (g_{bh}), impeding heat transfer between leaves and air. For five species, with trichome lengths of 135-780 µm, we transiently heated leaves with a radiative light source, measured the time constant for subsequent leaf cooling simultaneously in two adjacent leaf regions (with and without trichomes) with an IR camera, and inferred g_{bh} using an energy balance model. Cooling was slower in hairy leaf regions relative to bald regions, corresponding to a lower g_{bh} in hairy regions, by 2.4% to 39% across species. Contrary to prior theory, the resistance added by trichomes was unrelated to the depth of the hair layer (i.e., trichome height) across species. Simulations predicted that the reduction in g_{bh} by trichomes would influence energy balance and gas exchange rates by up to a few percent, with the direction and magnitude of such effects depending sensitively on environmental conditions.

Introduction

Leaf hairs, formally known as trichomes, are epidermal appendages on average present in >50% of species in given ecosystems and varying widely in morphology among and even within species (Perez-Estrada et al., 2000). Leaf hairs are thought to provide several functional roles. They provide mechanical protection against phytophagous insects (Levin, 1973; Dalin et al., 2008), and some plant species can produce leaf hairs with glandular secretion which also serve a defensive purpose (Werker, 2000). Leaf hairs can also provide protection from disease pressures such as downy mildew (Kortekamp and Zyprian, 1999). Leaf hairs also influence energy balance and gas exchange. The measured effect of hairs on leaf temperature varies, from warming up to several degrees C (Woolley, 1964; Ehleringer and Mooney, 1978; Ripley et al., 1999; Peng et al., 2015) to cooling in summer and warming in winter (Ehleringer and Mooney 1975). The overall effect of hairs on water use efficiency (WUE, the ratio of net photosynthetic rate to transpiration rate) differs across studies but is most commonly reported to be positive (Ehleringer and Mooney, 1978; Ripley et al., 1999). The influence of trichomes on leaf temperature and gas exchange arises from effects on reflectivity and the boundary layer. Trichomes can lower leaf absorptance to visible light (Wuenscher, 1970a; Holmes and Keiller, 2002) and provide protection from photoinhibition, ultraviolet radiation and overheating (Ehleringer and Mooney, 1978; Karabourniotis et al., 1992; Karabourniotis et al., 1995; Ntefidou and Manetas, 1996).

Trichomes are also thought to influence the diffusive exchange of heat and mass across the leaf boundary layer – that is, the zone adjacent to the leaf surface where wind speed is substantially reduced by friction with the leaf surface, and in which transport is therefore dominated by diffusion rather than by advection. Because diffusion is much slower than advection at macroscopic scales (e.g., over distances > ˜21 µm at a wind speed of just 1 m s^{-1}), the boundary layer slows heat and gas exchange between the leaf and air (Raschke, 1960; Grace and Wilson, 1976). It is most often assumed that hairs increase the effective thickness of the boundary layer by entraining a layer of relatively still air, and thereby impede heat and mass transport, and that boundary layer thickness relates to the height of the trichome canopy (Wuenscher, 1970a; Ehleringer and Mooney, 1978; Nobel, 2005). However, some have speculated the converse, on the premise that hairs break up air flow and thereby promote turbulence (Wolpert, 1962; Schreuder et al., 2001).

These contrary theoretical speculations on the influence of leaf trichomes on the boundary layer, and potentially on gas exchange, have have not been adequately tested experimentally. This may be partly because leaf boundary layer conductance is perceived to be very large relative to stomatal conductance (Nobel, 2005; Jones, 2014) and thus relatively unimportant. Indeed, many models assume leaf and air temperatures are always equal (Dong et al., 2017), which is equivalent to assuming boundary layer conductance is infinite (resistance is zero), so that leaf temperature is strongly coupled with air temperature. Yet many studies have reported large leaf-air temperature differences *in situ* (Leigh et al., 2017; Fauset et al., 2018; Guha et al., 2018; Xu et al., 2020): e.g., ΔT (leaf minus air) = +5.1 ± 2.1°C (mean ± SD) for 68 Proteaceae species (Leigh et al., 2017); –6 to +7 °C for three woody species in a tropical dryland (Dong et al., 2017); +3.7 to + 4.7 °C in wheat (Ehrler et al., 1978; Ayeneh et al., 2002); –4.1 to +4.1°C in almond canopies (Gonzalez-Dugo

et al., 2012). Leaf-air temperature difference is strongly influenced by boundary layer conductance because it directly influences both convective heat exchange and transpiration (and thus latent cooling).

Full resolution of precisely how trichomes affect the boundary layer has not been achieved, because of the technical difficulty of estimating boundary layer conductance experimentally in real leaves, rather than in physical models of leaves. It is common, for example, to estimate boundary layer conductance to water vapor in a gas exchange chamber using a wet filter paper or other wet fabric surface, to represent a leaf without an epidermis and thus without stomatal resistance (Monteith and Unsworth, 2013). Another approach, based on using rigid, heated metal plates, contributed to the validation of phenomenological equations relating g_{bh} to wind speed and to leaf size (specifically, the characteristic dimension related to downwind width) (Gates, 1968; Nobel, 1975; Schuepp, 1993; Brenner and Jarvis, 1995; Schlichting and Gersten, 2017). Another set of methods is based on surface treating leaf surfaces with water or a water-impermeable substance to modulate the contribution of evaporation to energy balance (Impens, 1966; Impens et al., 1967; Linacre, 1972; De Parcevaux and Perrier, 1973; Paw U and Daughtry, 1984). While potentially powerful, each of those approaches is difficult to apply to the specific question of how leaf hairs affect boundary layer conductance. The most direct experimental test of this question was performed by Wuenscher (1970), who examined how the removal of leaf hairs affected transpiration rate in *Verbascum thapsus* . Although Wuenscher concluded that hairs reduced boundary layer conductance, later reanalysis by Parkhurst (1976) suggested that cuticular damage caused by shaving led to enhanced transpiration and evaporative cooling, which confounded Wuenscher's results.

Dynamic thermography – heating a leaf and then measuring its rate of cooling by convection (Jones, 2014) – can quantify boundary layer conductance independent of the effect of hairs on light absorption. Dynamic thermography using infrared cameras has recently been used successfully to quantify both boundary layer conductance (Albrecht et al., 2020) and stomatal conductance (Vialet-Chabrand and Lawson, 2019) in intact leaves. Here we adapt and extend the approach of Albrecht*et al* . (2020) to quantify the influence of leaf hairs on boundary layer conductance to heat (g_{bh}; see Table 1 for a list of symbols) in five broadleaved species, by measuring the time constant for leaf cooling (τ) after transient radiative heating in leaf patches with hairs and without hairs and then inferringg_{bh} from τ using a dynamic energy balance model, accounting for stomatal conductances measured in each patch. We hypothesized that leaf hairs will add a component of transport resistance that is proportional to the depth of the hair layer, thereby reducing g_{bh} compared to an otherwise similar leaf surface without leaf hairs.

Methods and Materials

Plant material

We collected branches from three to five individuals of each of four woody species varying strongly in leaf morphology and trichome depth (Table 2) growing on the UC Davis campus (Davis, CA, 35.54°N, 121.75°W), recut them under water upon return to the laboratory, and allowed them to equilibrate for at least one hour in darkness before beginning measurements. For the fifth species (*Solanum lycopersicon* , SOLY), we compared leaves from five plants from each of two mutant genotypes (*Wo* , wooly;*h* , hairless) in the same genetic background (known as 'Ailsa Craig'). SOLY seeds were provided by the UC Davis Tomato Genetics Resource Center. We grew SOLY plants under LED lights in the laboratory for a month before experiments.

Dynamic infrared thermography

Overview . We quantified the dynamics of leaf temperature using an infrared camera (ICI 8640P, ICI Inc., Beaumont, TX) after transient radiative warming. The leaf was illuminated for 5-8 sec with a 275 W near-infrared heat lamp (model ZB:IL04-06, Serfory), causing its temperature to increase by approximately 15 – 40 K. The mean temperature in each of two regions of interest ("patches"), one with hairs and one without, was then recorded with the infrared camera at 5 Hz until temperature had ceased to decline noticeably ($<$ 60 sec). Wind speed was measured with a hot-wire anemometer (FMA903R-V1, Omega, Stamford, CT) mounted 3 cm below the leading edge of the leaf. Air temperature was measured with a fine-wire type-T thermocouple (TT-T-36, Omega) mounted on the anemometer. Each such "cooling curve" experiment was

repeated 3-5 times for each of 5-6 leaves in five species (Table 2).

Leaf and patch preparation . Each leaf was excised from the plant shortly before measurements, and vacuum grease (DC 976, Dow-Corning, Midland, MI) was applied to the cut petiole to minimize water loss. The leaf was then placed in a mesh of fishing lines to secure it for measurements (an example, not from an actual experiment but set up for demonstrative purposes, is shown in Fig S1), such that the lamina was parallel to the direction of the wind flow. The mesh had a 45-degree opening in the direction facing incoming airflow; all temperature measurements were performed on regions located in that gap, to ensure that the fishing lines did not influence airflow upstream of the patches. We selected two leaf patches: one with leaf hairs and one without. In three species (OLEU, MAGR and PLOC), we were able to remove hairs from a patch, either by gently scraping the leaf surface with a razor blade oriented nearly perpendicular to the surface (OLEU and MAGR), or by gently rubbing the hairs off using a thumb and forefinger (PLOC). Although we were unable to remove hairs from POTO leaves by hand, this species exhibits extreme variation in trichome density among leaves, even of similar age. Thus, for POTO, we mounted two leaves in the fishing line mesh – one hairy and one hairless. We did the same for SOLY, comparing mutants with excessive hairs or without hairs. For each experiment with POTO and SOLY, we chose two leaves of similar size and shape; in the case of POTO, both leaves were always sampled from the same branch.

A rectangular region of interest (ROI) was located in each patch using the camera software. The ROIs were equal in size (approximately 5 x 5 mm) and were typically positioned with around 3 mm of distance between the ROI and the leading edge of the leaf. The patches could not always be located at precisely the same distance from the leaf edge across experiments, due to the practical difficulty of finding a suitable area in each leaf where hairs could be removed without damaging the underlying tissue. However, within each experiment, the two patches were always located at the same distance from the leaf edge as one another, and were placed in locations such that the adjacent leaf edge was oriented at a similar angle with respect to the direction of airflow for both patches. This ensured that heat transfer properties could be directly compared between the two patches in a given experiment.

Wind . Wind was generated by CPU fans arrayed horizontally in the leaf plane and located at one end of a 2-m long and 25-cm diameter cylindrical wind tunnel made of mylar-covered bubble wrap (Reflectix; Reflectix, Inc., Markleville, IN). The leaf was located approximately 10 cm from the other end of the wind tunnel. Tests with the anemometer showed that wind speed did not vary with position within the range of locations where the leaf patches were located, nor between the leaf plane and the location 3 cm below it where the anemometer was located during experiments. For each species, we adjusted the number of CPU fans and/or their voltage input to produce the highest wind speed that would not cause noticeable flapping or other leaf movement during the experiment. PLOC, SOLY and POTO leaves were too physically unstable at the higher wind speed generated using four CPU fans; most of the results described below were therefore limited to lower wind speeds generated using two CPU fans. Wind speed was steady during each experiment (average SD = 0.029 m s^{-1}), and wind speed varied between 0.76 and 2.13 m s^{-1} among experiments.

Procedural details . Inference of leaf boundary layer conductance from temperature dynamics (see *Theory* below) requires the radiative environment of the leaf to be constant during the experiment, because this eliminates incoming radiation terms from the derivative of leaf temperature with respect to time, leaving dependences only on factors that can be more easily measured (namely leaf temperature, air temperature, stomatal conductance and leaf heat capacity). We therefore designed the experimental apparatus (Figure 1) to ensure that incoming radiation was constant during each cooling curve. First, the heat lamp was mounted on a large articulating arm, which allowed an operator to move the lamp away from the leaf after heating, into a position located in the same plane as the leaf but about 1 m away. We also attached a piece of Reflectix to the side of the lamp head that was facing the leaf when in the latter position, to block radiation. Second, we used an A-frame Reflectix shield mounted over the camera to shield the camera and leaf from any fluctuations in incoming infrared radiation caused by people operating the apparatus. Third, the camera was moved out of position using a sliding boom stand (model BBB, Amscope, Irvine, CA) while heating the leaf, so that the camera would not be heated by the lamp. Fourth, during leaf heating, we shielded the

air temperature and wind speed sensors (which were located 3 cm below the leading edge of the leaf), as well as other objects below the leaf, from the heat lamp with a plastic plate covered with aluminum foil and mounted on a sliding boom stand. We then moved this shield out of the way after heating the leaf, and simultaneously rotated the lamp out of the way using its articulating arm, and moved the camera back into place using its sliding boom stand. The transition from heating to measuring took approximately one second. Figures 1b and 1c illustrate the positions of each component of the apparatus during leaf heating and measurement, respectively.

Black-body calibration . To ensure that leaf temperatures measured by infrared thermography were commensurable with air temperatures measured with the fine-wire thermocouple, which allowed modeling of the leaf-air temperature difference (see *Theory*), we calibrated the infrared camera against a black-body reference before each cooling curve. The black-body consisted of a basketball that had been cut in half, the two halves inverted (which increased their rigidity), coated internally with graphite with the aid of spray adhesive, reassembled using duct tape, and placed into an insulating foam box covered in Reflectix. The black-body contained a fine-wire thermocouple previously calibrated to match the fine-wire thermocouple used to measure air temperature below the leaf. A square 2 x 2 cm window was cut into both the basketball and the foam box. The black-body was located such that the camera's field of view was focused on the window into the black-body when the camera was moved out of the way for leaf heating. We recorded the mean IR temperature in the black-body window for 2 seconds, computed a correction factor by comparing that measurement with the output of the thermocouple located in the black-body, and applied this correction factor to IR temperature records for the subsequent cooling curve.

Theory: inference of boundary layer conductance from leaf temperature dynamics

Leaf boundary layer conductance to heat (g_{bh}) can be estimated from the time constant for leaf cooling (τ) using a model of leaf energy balance, in which the rate of change of leaf heat content, and thus temperature, is proportional to the difference between energy gains and losses (radiative, convective and latent) and inversely proportional to the leaf's heat capacity. A full derivation is presented in Supporting Information Methods S1; only key results are given here. The derivative of leaf temperature (T , K) with respect to time (t) is

$$\frac{\mathrm{dT}}{\mathrm{dt}} = \frac{Q - 2\epsilon\sigma T^4 - c_{\mathrm{pa}} g_{\mathrm{bh}} (T - T_a) - \lambda g_{\mathrm{tw}} \Delta w}{k} , \qquad Eqn\ 1$$

where k is the leaf heat capacity (J m^{-2}K^{-1}), Q is absorbed radiation, including both shortwave and longwave (J m^{-2} s^{-1}),ϵ is leaf thermal emissivity, σ is the Stefan-Boltzmann constant (5.67[?]10^{-8} J m^{-2}s^{-1}), c_{pa} is air heat capacity (29.2 J mol^{-1} K^{-1}),g_{bh} is (2-sided or whole-leaf) boundary layer conductance (mol m^{-2} s^{-1}),T_{a} is air temperature in kelvins, λ is the latent heat of vaporization (44000 J mol^{-1}),g_{tw} is total leaf conductance to water vapor (mol m^{-2} s^{-1}), and Δw is the leaf-to-air water vapor mole fraction difference (mol mol^{-1}). Δw equals$w_{\mathrm{s}}(T) - w_{\mathrm{a}}$, where$w_{\mathrm{s}}$ and w_{a} are saturated and ambient water vapor mole fractions, respectively, the former calculated at the leaf temperature. The terms that are nonlinear in leaf temperature (T^4 and$w_{\mathrm{s}}(T)$) can be expressed in terms of the leaf-to-air temperature difference, δ [?] $T - T_{\mathrm{a}}$, by approximations given in Supporting Information Methods S1 (Eqns S2-S6). Assuming $T_{\mathrm{a}}$is constant, the result is a differential equation for δ :

$$k\frac{\mathrm{d}}{\mathrm{dt}} = a - \beta\delta , \qquad Eqn\ 2$$

where a [?] $Q - 2\epsilon\sigma T_{\mathrm{a}}^4 - \lambda\gamma_{\mathrm{tw}} D_{\mathrm{a}}$, b [?] $8\epsilon\sigma T_{\mathrm{a}}^3 + c_{\mathrm{pa}} g_{\mathrm{bh}} + \lambda\gamma_{\mathrm{tw}} s$, and s is the derivative ofw_{s} with respect to T . Integrating Eqn 2 leads to the solution

$$\delta(t) = \delta_f - (\delta_f - \delta_i) e^{-\frac{t}{\tau}} , \qquad Eqn\ 3$$

where $\delta_{\,i}$ and $\delta_{\,f}$ are values of δ at $t = 0$ and in the limit of large t , and the cooling time constant, τ , equals $k\ /b$. τ is thus a function of $g_{\,bh}, T_{\,a}$, stomatal conductance (via$g_{\,tw}$) and leaf heat capacity (k). We fitted Eqn 3 to each cooling curve using the nls() function in R. To provide the algorithm with initial estimates for the parameters ($\delta_{\,i}$, $\delta_{\,f}$ and τ), for$\delta_{\,i}$ we used the first three measurements ofδ (which spanned the first 0.6 s of cooling), for$\delta_{\,f}$ we used the minimum value of δ (at or near the end of the cooling curve), and for τ we used the observed halftime for cooling (the time at which δ first dropped below $\delta_{\,f} + 0.5(\delta_{\,i} - \delta_{\,f})$) divided by the natural logarithm of 2. We used the mean value of air temperature during each cooling curve as$T_{\,a}$, and computed s at the midpoint between leaf and air temperatures when δ was halfway between$\delta_{\,i}$ and $\delta_{\,f}$. The resulting fitted model produced an estimate for τ for each patch in each cooling curve. We then estimated $g_{\,bh}$ fromτ by solving $\tau = k\ /b = k\ /(8\epsilon\sigma T_{\,a}{}^3 + c_{\,pa} g_{\,bh} + \lambda\gamma_{\,tw} s\ )$ for $g_{\,bh}$ to give

$$g_{\mathrm{bh}} = \frac{\frac{k}{\tau} - 8\epsilon\sigma T_a^3 - \lambda g_{\mathrm{tw}} s}{c_{\mathrm{pa}}} \quad . \qquad Eqn\ 4$$

To estimate $g_{\,tw}$ for application to Eqn 4, we measured surface conductance to water vapor, $g_{\,sw}$, in each patch immediately before each experiment, for the abaxial leaf surface, using a leaf porometer (AP4, Delta-T devices, Cambridge, UK).$g_{\,tw}$ is not independent of$g_{\,bh}$, because $g_{\,tw}$ includes components of $g_{\,bh}$ relevant to the transpiring surface(s); accounting for this interaction leads to a quadratic expression for $g_{\,bh}$ (Eqn S15). We assumed that$g_{\,sw}$ at the adaxial surface was either equal to the value measured by porometry at the abaxial surface (in amphistomatous species) or zero (in hypostomatous species), and that the resistance added by hairs was either equal on both leaf surfaces (in SOLY, which had hairs on both surfaces) or was zero on the adaxial surface (for the other species).

Estimation of $g_{\,bh}$ as described above also requires estimates of leaf thermal emissivity (ϵ) and leaf heat capacity (k). We assumed $\epsilon = 0.98$ (e.g., Chen, 2015), and addressed the effect of uncertainty in ϵ as described below. We estimated k as (4.184[?]WM + 1.5[?]DM)/LA, where WM, DM and LA are leaf water mass, dry mass and leaf area, respectively; this assumes heat capacities of 4.184 J g^{-1} K^{-1} for water and 1.5 J g^{-1} K^{-1} for leaf dry matter (Samarasekara and Coorey, 2011). We measured WM, DM and LA as follows: immediately after each experiment, we photographed each leaf to measure leaf area in ImageJ, then weighed the leaf using a 5-point digital balance (XS225DU, Mettler-Toledo, Columbus, OH), dried it in a drying oven at 65 °C for at least 24 hours, and then reweighed it after mass stopped changing. DM was taken as the final leaf mass, and WM as the difference between fresh and dry masses.

Effect of uncertainty in thermal emissivity

We did not measure leaf thermal emissivity (ϵ), but assumed a fixed value of 0.98. To assess how a systematic difference in ϵbetween bald and hairy patches would have affected our results, we simulated cooling curves assuming ϵ was between 0.94 and 0.99 in bald patches but 0.98 in hairy patches, or vice versa. Additional details are provided in Supporting Information Methods S2. This analysis found that uncertainty in ϵ would have negligible effect on inferred differences in $g_{\,bh}$ between hairy and bald patches (Figs S2 and S3).

Effect of lateral heat conduction between adjacent patches

We assessed the potential influence of lateral heat conduction between adjacent bald and hairy patches in the same leaf during cooling curves (Supporting Information Methods S3). Our analysis suggests that the rate of lateral heat conduction between patches was between 250 and 2,000 times smaller than the rate of convective heat loss to the air, indicating that lateral heat conduction was unlikely to have substantially influenced our results.

Resistance added by hair layer

The resistance added by leaf hairs, $r_{\,h}$, can be estimated from the difference in boundary layer resistance between bald and hairy patches, as described in Supporting Information Methods S4. Because estimating $r_{\,h}$ requires a value for an unknown parameter – the ratio (β), between adaxial and abaxial leaf surfaces, of the component of boundary layer resistance that is not caused by hairs – we inferred $r_{\,h}$ at a range of

values of β (Fig S4) and presented results below assuming a nominal value of $\beta = 1$. We compared the resulting values of r_{h} with theoretical predictions that assumed leaf hairs entrain a layer of still air equal to the depth (d_{h}) of the hair layer; the diffusive resistance through such a layer would be $r_{\mathrm{h}} = d_{\mathrm{h}}[?]RT/D_{\mathrm{ha}}P$, where R is the gas constant (8.31446 Pa $m^3 mol^{-1}$ K^{-1}), T is temperature (298.15 K), D_{ha} is the binary diffusivity for heat in air ($2.36[?]10^{-5}$ $m^2 s^{-1}$), and P is the atmospheric pressure (10^5 Pa). We measured d_{h} by microscopy in fresh leaf sections for three leaves per species, as the distance between the exterior edge of the trichome layer and the leaf cuticle at the base of the trichome (Table 2). We measured trichome length in SOLY (genotype *Wo*) from images in Gasparini *et al.* (2021); the results were consistent with another study on the same genotype (Zhang et al., 2020).

Effects of leaf hairs on leaf temperature, gas exchange and water use efficiency

To quantify how leaf hairs would influence CO_2 and H_2O exchange, water use efficiency (WUE, the ratio of CO_2 and H_2O exchange rates) and leaf temperature, we simulated gas exchange and leaf temperature for a range of combinations of parameters (resistance added by hairs, leaf size, wind speed, stomatal conductance, incident radiation, air temperature and ambient humidity), by combining a steady-state version of the dynamic leaf energy balance model that we used to estimate g_{bh} with a widely used biochemical model of photosynthesis (see Supporting Information Methods S5 for details).

Results

We measured a total of 147 pairs of cooling curves (49 in OLEU, 50 in MAGR, 15 in PLOC, 15 in SOLY and 18 in POTO) for bald and hairy leaf patches. Figure 2 shows a typical experiment for an OLEU leaf. In that experiment, after transient radiative heating, the temperature of each patch declined from approximately 30 K above air temperature to a final value just below air temperature, in each case closely following an exponential model (Eqn 3) fitted to the data. In this example, the bald patch was initially warmed to a slightly greater temperature than the hairy patch, presumably due to the greater albedo contributed by the hairs (albedo was not measured); thus, the bald patch cooled more rapidly in absolute terms (i.e., with a greater rate of change of temperature). Yet, the intrinsic kinetics of cooling were also faster in the bald patch – that is, the time constant for cooling was shorter ($\tau = 9.79$ s vs 10.94 s for the hairy patch); indeed, despite having begun at a higher temperature, after about 10 seconds the temperature of the bald patch dropped below that of the hairy patch. In 141 of 147 experiments (96%), τ was smaller (cooling was faster) in the bald patch than in the hairy patch (Fig 3). The mean ratio of τ between bald and hairy patches within species ranged from 0.578 ± 0.050 (mean $\pm$ SE; SOLY) to 0.957 ± 0.007 (MAGR).

We inferred leaf boundary layer conductance to heat (g_{bh}) by applying measured values of τ, air temperature, leaf surface conductance to water vapor (g_{sw}), and leaf heat capacity (k) to Eqn 4. The relationship between g_{bh} and τ was fairly consistent within most species (Fig 4), because the two factors that could create divergence in that relationship –g_{sw} and k – were fairly similar among leaves for a given species (Tables 2 & 3) (though one PLOC leaf had a much lower water content, and hence lower heat capacity, than the other leaves of that species; that leaf corresponds to the group of blue symbols closest to the origin in Fig 4). Because the leaves had been acclimated in darkness for at least an hour before measurement, g_{sw} (measured by porometry before each cooling experiment) was generally low (Table 3) and did not increase after trichome removal by shaving for the two species subjected to this treatment (OLEU and MAGR) (Table 3). For the two species for which we compared different leaves with and without hairs (SOLY and POTO), g_{sw} was marginally greater in hairy leaves than in bald leaves (Table 3). In the fifth species, PLOC, g_{sw} was on average greater in bald than in hairy patches (0.072 ± 0.005 mol m^{-2} s^{-1}[bald] vs 0.043 ± 0.012 mol $m^{-2} s^{-1}$ [hairy]). Across all species and experiments, g_{sw} was slightly but significantly lower in bald patches than in hairy patches ($p < 0.0001$; linear mixed model of g_{sw} with species and hair condition as fixed effects and leaf as a random effect); Tukey's post hoc tests also found this result also held within each individual species except PLOC ($p < 0.0001$). Our estimation of g_{bh} from τ accounted for observed differences in g_{sw} between patches (discussed below), and our finding of faster cooling in bald patches could thus not be attributed to g_{sw} differences.

Boundary layer conductance varied among leaves and experiments, from 2.33 mol m^{-2} s^{-1} (for a hairy patch in a POTO leaf) to 8.12 mol m^{-2} s^{-1}(for a bald patch in a PLOC leaf) (Fig 5). Boundary layer conductance was greater in the bald patch than in the hairy patch in nearly all experiments (138 of 147 cases; 94%) (Fig 5). Excluding a single outlier leaf of POTO (the three green points farthest from the 1:1 line in Fig 5), the increase of boundary layer resistance (decrease ing_{bh}) due to trichomes ranged from 2.4 ± 1.4% (mean ± SE; PLOC) to 38.7 ± 6.1% (POTO) (Fig 6).

Hair layer depth varied 6-fold across species (Table 2). The predicted resistance contributed by hairs (r_h, calculated from hair layer depth by assuming hairs entrained a layer of still air equal in thickness to the hair depth) was unrelated to the value ofr_h estimated from experimentally observed differences in g_{bh} between bald and hairy patches (Fig 7). The latter estimates, however, depended sensitively on the assumed ratio (β) of boundary layer resistance between the adaxial and abaxial surfaces in the absence of hairs (Fig S4); the values shown in Fig 7 assumed a nominal value of $\beta = 1$.

Our modelling predicted that reduction of g_{bh} by leaf hairs in most cases reduced gas exchange rates, though to a greater extent for transpiration than for CO_2 assimilation (cf. Figs 8a,b). In most cases, trichomes caused predicted declines of approximately 0.25 – 0.50% in assimilation rate, but 1 – 2% in transpiration rate, leading to increases of 0 – 1% in WUE. The main exception was at low temperature, when hairs were predicted to increase gas exchange rates and decrease WUE. The effect of trichomes on WUE was predicted to be greater (1) when evaporative demand (VPD) is high, whether due to low vapor pressure or high air temperature, (2) when stomatal conductance is large compared to boundary layer conductance, (3) when PPFD is subsaturating, and (4) in small leaves, provided air temperature is high (Fig 8).

Discussion

This study provides the first unambiguous experimental proof that leaf hairs reduce the boundary layer conductance for heat transfer between leaves and the air (g_{bh}). Our approach was carefully designed to exclude all potentially confounding influences: we inferred g_{bh} in bald patches and in otherwise identical hairy patches from the time constant for cooling following transient radiative heating, accounted for differences in leaf surface conductance to water vapor and leaf heat capacity, and ensured that the radiative environments of each patch were identical and constant over time. Cooling was faster and boundary layer conductance was greater in the bald patch than in the hairy patch in nearly all experiments, by 2.4 to 38.7% (means within species). This finding could not be attributed to differences in stomatal conductance or other components of energy balance between patches. Our results thus validate the hypothesis that leaf hairs slow convective heat exchange between leaves and air.

Several previous studies have examined the effects of leaf hairs on leaf energy balance or gas exchange, though none was able to directly quantify the effect of hairs on boundary layer conductance in intact leaves in isolation from potential confounding factors. Benz and Martin (2006) found no correlation between trichome cover and gas exchange rates across 12 *Tillandsia* species, and concluded that hairs had negligible influence on boundary layer conductance; yet, other factors that differed across the 12 species may have confounded the observed differences in gas exchange rates. Wuenscher (1970b) observed higher leaf temperatures and lower transpiration rates in shaved versus unshaved leaves of *Verbascum thapsus* , and attributed these differences to a 90-fold increase of boundary layer resistance by hairs. However, Parkhurst (1976) reassessed Wuenscher's results and concluded that hair removal would likely have increased boundary layer resistance two-fold at most, and suggested a role for cuticular or epidermal damage caused by hair removal; differences in stomatal conductance may also have played a role. Ripley et al (1999) measured surface conductance to water vapor by gas exchange before and after removal of hairs from*Arctotheca populifolia* leaves, and inferred that the hairs generated a resistance of around 0.2 m^2 s mol^{-1}; however, as in Wuenscher's (1970) study, those results could have been influenced by other unobserved changes in leaf surface vapor transport caused by hair removal. Woolley (1964) observed a substantial reduction in wind speed near the surface (both above and within the hair layer) of hairy soybean leaflets as compared to shaved leaflets, which is consistent with an increase in the effective boundary layer thickness and a reduction in g_{bh}. Measurements of water loss were more ambiguous: variability obscured any effect of hairs in excised, living leaflets, whereas shaving increased

transpiration rate by 21% in leaflets that had been killed by boiling. Meinzer and Goldstein (1985) simulated effects of hairs on energy balance in *Espletia timotensis* by assuming hairs entrained a layer of still air equal to their depth and that hairs did not affect absorptance; their simulations reasonably matched observations of greater leaf temperatures in hairy as compared to partially-shaved leaves. Amada et al. (2021) observed lower *in situ* leaf temperatures in shaved versus hairy leaves of *Metrosideros polymorpha* ; having verified that surface conductances to water vapor did not differ between the two treatments, the authors attributed the result to reduction in g_{bh}, and thus in convective cooling. That result could also have arisen from effects of leaf hairs on radiation absorption, although hairs in *M. polymorpha* are light in color and thus probably reduced radiation absorption rather than the converse.

In the present study, we directly quantified g_{bh}itself in hairy and bald leaf patches, and eliminated all factors that could have confounded the results of previous studies described above: (1) We eliminated the confounding influence of differences in light absorption by using dynamic IR thermography rather than steady-state temperature to infer differences in g_{bh}, which enabled us to estimate g_{bh} *per se* despite any differences in light absorption. (2) We eliminated the confounding influence of differences in leaf size and shape between bald and hairy leaves by choosing adjacent bald and hairy patches identical in size and position relative to the leading edge of the leaf, and ensured identical wind speeds by measuring both patches simultaneously in the same air stream. (3) We eliminated the confounding effects of transplanting hair layers or boiling leaves by measuring only intact leaves from which hairs had been either left in place or removed. (4) We eliminated the confounding influence of differences in stomatal conductance by measuring surface vapor conductance directly in each patch with a porometer immediately before measurements and incorporating those data into our inference of g_{bh}. Surface conductance was very low in general, but was marginally lower on average in bald patches than in hairy patches, ruling out evaporative cooling as a general explanation for faster cooling in bald patches.

Our results do not appear to confirm the theoretical prediction that hairs add a resistance, r_h, proportional to the depth of the hair layer (d_h). While hair depth and theoretical r_h varied nearly 6-fold across species in this study (from 0.04 to 0.80 m^2 s mol^{-1} for r_h), our experimental estimates of r_h – based on observed differences in g_{bh} between bald and hairy patches – were unrelated to theoretical predictions (Fig 7), although they spanned a similar range. The experimental estimates also depended sensitively on the value of an unknown parameter: the ratio (β) between the boundary layer resistances at the adaxial and abaxial surfaces in the absence of hairs. It may seem reasonable to assume β [?] 1. However, in three of our study species (MAGR, OLEU and SOLY), the edges of each leaf had a slight downward curl that may have slightly sheltered the abaxial surface from wind, which could have increased boundary layer resistance at that surface independent of hairs, making β less than 1.0. A similar effect was reported by Grace and Wilson (1976), who found lower wind speeds just behind the downward-curled leading edge of the abaxial surface in *Populus* × *euramericana* . $\beta <$ 1 would bring the results for r_h in OLEU and MAGR closer to the theoretical predictions: observed and theoretical r_h would match at $\beta = 0.47$ for MAGR and $\beta = 0.67$ for OLEU (Fig S4). In summary, our data suggestr_h is at best weakly related to hair layer depth, but is probably on the same order of magnitude as theoretical predictions based on hair layer depth.

Our results also initially appear inconsistent with modeling by Schreuder et al. (2001), which suggested that leaf hairs may*enhance* g_{bh} by promoting turbulence near the leaf surface. However, turbulence was predicted to emerge only above a critical windspeed that depended on trichome height; e.g., for 2.5 cm leaves with 500 µm trichomes, the critical windspeed was 2.18 m s^{-1}, and the critical windspeed increased as trichome height decreased and leaf size increased. In our experiments, wind speed was below 2 m s^{-1} in most experiments, trichomes were shorter than 300 µm in all species except SOLY (Table 2), and leaves were >> 2.5 cm wide except in OLEU. Thus, our data neither contradict nor confirm the predictions of Schreuder et al. (2001). It is interesting to note, however, that the largest deviation between theoretical and experimental estimates ofr_h in this study was in SOLY, which also had the longest trichomes by far. The fact that experimentalr_h was less than half the theoretical prediction for SOLY, regardless of what value of β we assumed, may hint at promotion of turbulence by tall hairs as proposed by Schreuder et al. (2001).

We could not rigorously scale up our estimates ofg_{bh} from the patch scale to whole leaves – the estimates reproted here refer only to the individual patches of leaf measured within each experiment – for three reasons. First, we could not locate patches at a constant distance from the leaf edge across experiments, due to the difficulty of finding leaf patches that we could successfully shave without damaging the leaf. Second, it was impossible to remove hairs from entire leaves in most cases. Third, our results did not validate the estimate of hair-layer resistance from hair-layer depth; had they done so, then we could have concluded that the effect of hairs is independent of leaf size, in which case we could merely add a calculated hair-layer resistance to predictions from existing models ofg_{bh} in relation to leaf size and wind speed. For example, prior theory predicts that g_{bh} is proportional to the square root of the ratio of wind speed (v_w, m s^{-1}) to leaf size (d_l, m), thus: g_{bh} [?] $0.267(v_w/d_l)^{0.5}$, where g_{bh} is a whole-leaf (two-sided) value in mol m^{-2} s^{-1} (Gates, 1968; Nobel, 1975). In the context of that theory, the range of % decreases ing_{bh} that we observed (means of 2.4 to 39% across species) correspond to the effect, predicted by the theory, of a 4.9 – 93% increase in leaf size or a 4.6 – 48% decrease in wind speed. An important caveat is that our data apply only to leaf patches located 2 – 6 mm from the leading edge of a leaf. Given that the wind speed at a given position above the leaf surface declines progressively with distance from the leaf edge (e.g., Grace and Wilson, 1976), the boundary layer resistance in the absence of hairs likewise increases with distance from the leaf edge, which would make hair-layer resistance a smaller proportion of the total resistance in locations farther from the leaf edge. Thus, had we located patches farther from the leaf edge, we may have found smaller *percent* increases in boundary layer resistance due to hairs.

Authors have speculated for decades about how leaf hairs affect photosynthesis (A) and transpiration (E) via boundary layer conductance. Hairs have a wide range of reported effects on gas exchange (e.g., Ehleringer and Mooney, 1978; Baldocchi et al., 1983; Ripley et al., 1999), but it is typically difficult to disentangle the effect mediated by g_{bh} from other effects of hairs, such as on radiation balance. For example, a seminal study by Ehleringer and Mooney (1978) reported large suppression of both $A$and E by hairs in *Encelia farinosa* as compared to its close hairless relative *E. californica* , though these effects were largely driven by increased reflectance due to hairs; photosynthesis rates were similar with or without hairs after correcting for differences in light absorption, indicating little or no effect of hairs on boundary layer resistance. Amada et al. (2017) found small differences in gas exchange rates in *M. polymorpha* , consistent with the small (< 10%) increases in total CO_2or H_2O transport resistance due to trichomes predicted from the thickness of the trichome layer. Our modeling suggests theg_{bh}-mediated effects of hairs on gas exchange should depend sensitively on conditions. A hair-layer resistance of 0.1 m^2 s mol^{-1} – roughly the value we estimated for OLEU – would change instantaneous WUE by -1.7% to +2.9% depending on conditions, according to our model. For example, hairs would increase WUE by nearly 2% at a stomatal conductance of 0.5 mol m^{-2} s^{-1} or by 1.5% at a PPFD of 250 µmol m^{-2} s^{-1}, or decrease WUE by 1.5% in a 1 mm leaf at 10°C (Fig 8). Generally, hairs should tend to improve WUE when stomatal conductance, air temperature or VPD is high or when PPFD is subsaturating. Hairs should influence WUE to a greater degree in small leaves, though the direction of the effect depends on air temperature.

Conclusion

We quantified boundary layer conductance to heat transfer in matched patches or leaves, with or without leaf hairs (trichomes), in five broadleaved species, using dynamic infrared thermography. Our results provide the first direct experimental proof for the long-standing hypothesis that leaf hairs impede convective heat exchange between leaves and the adjacent air. Boundary layer conductance was 2 – 39% greater in patches or leaves without hairs than in the presence of hairs. Leaf hair layer depth did not predict increases in boundary layer resistance due to the presence of hairs, in contrast with prior theoretical predictions, but these results were uncertain due to uncertainty in the ratio of boundary layer resistance between the two leaf surfaces in the absence of hairs. This study supports the use of dynamic IR thermography as a viable, practical technique for studying boundary layer conductance in real leaves.

Acknowledgements

This work was supported by the National Science Foundation (Award #1951244) and the USDA National

Institute of Food and Agriculture (Hatch Project 1016439). The authors thank Matthew Gilbert and Kyaw Tha Paw U for helpful feedback on an earlier draft.

Literature cited

Albrecht H, Fiorani F, Pieruschka R, Müller-Linow M, Jedmowski C, Schreiber L, Schurr U, Rascher U (2020) Quantitative Estimation of Leaf Heat Transfer Coefficients by Active Thermography at Varying Boundary Layer Conditions. Front Plant Sci **10** : 1684

Amada G, Kosugi Y, Kitayama K, Onoda Y (2021) Roles of leaf trichomes in heat transfers and gas-exchange characteristics across environmental gradients. Authorea (preprint)

Amada G, Onoda Y, Ichie T, Kitayama K (2017) Influence of leaf trichomes on boundary layer conductance and gas-exchange characteristics in Metrosideros polymorpha (Myrtaceae). Biotropica **49** : 482–492

Ayeneh A, Van Ginkel M, Reynolds M, Ammar K (2002) Comparison of leaf, spike, peduncle and canopy temperature depression in wheat under heat stress. Field Crops Research **79** : 173–184

Baldocchi D, Verma S, Rosenberg N, Blad B, Garay A, Specht J(1983) Leaf Pubescence Effects on the Mass and Energy Exchange Between Soybean Canopies and the Atmosphere 1. Agronomy Journal **75** : 537–543

Benz BW, Martin CE (2006) Foliar trichomes, boundary layers, and gas exchange in 12 species of epiphytic Tillandsia (Bromeliaceae). Journal of plant physiology **163** : 648–656

Bernacchi C, Pimentel C, Long SP (2003) In vivo temperature response functions of parameters required to model RuBP-limited photosynthesis. Plant, Cell & Environment **26** : 1419–1430

Bernacchi CJ, Singsaas EL, Pimentel C, Portis ARJ, Long SP(2001) Improved temperature response functions for models of Rubisco-limited photosynthesis. Plant, Cell and Environment **24** : 253–259

Brenner AJ, Jarvis PG (1995) A heated leaf replica technique for determination of leaf boundary layer conductance in the field. Agricultural and Forest Meteorology **72** : 261–275

Brutsaert W (1975) On a derivable formula for long-wave radiation from clear skies. Water resources research **11** : 742–744

Buckley TN, John GP, Scoffoni C, Sack L (2017) The Sites of Evaporation within Leaves. Plant Physiol **173** : 1763–1782

Buckley TN, Martorell S, Diaz-Espejo A, Tomas M, Medrano H(2014) Is stomatal conductance optimized over both time and space in plant crowns? A field test in grapevine (Vitis vinifera). Plant, cell & environment **37** : 2707–2721

Caemmerer S, Farquhar GD (1981) Some relationships between the biochemistry of photosynthesis and the gas exchange of leaves. Planta**153** : 376–387

Chen C (2015) Determining the leaf emissivity of three crops by infrared thermometry. Sensors **15** : 11387–11401

Dalin P, Agren J, Bjorkman C, Huttunen P, Karkkainen K (2008) Leaf Trichome Formation and Plant Resistance to Herbivory. *In* A Schaller, ed, Induced Plant Resistance to Herbivory. Springer Netherlands, Dordrecht, pp 89–105

De Parcevaux S, Perrier A (1973) Bilan energetique de la feuille. Application de l'etude des cinetiques de temperature a la determination des resistances aux flux gazeux. UNESCO **5** : 127–135

Dong N, Prentice IC, Harrison SP, Song QH, Zhang YP, Sykes M(2017) Biophysical homoeostasis of leaf temperature: A neglected process for vegetation and land-surface modelling. Global Ecol Biogeogr**26**

: 998–1007

Ehleringer JR, Mooney HA (1978) Leaf hairs: Effects on physiological activity and adaptive value to a desert shrub. Oecologia**37** : 183–200

Ehrler W, Idso S, Jackson RD, Reginato R (1978) Wheat canopy temperature: relation to plant water potential 1. Agronomy Journal**70** : 251–256

Farquhar GD, von Caemmerer S, Berry JA (1980) A biochemical model of photosynthetic CO2 assimilation in leaves of C3 species. Planta**149** : 78–90

Fauset S, Freitas HC, Galbraith DR, Sullivan MJP, Aidar MPM, Joly CA, Phillips OL, Vieira SA, Gloor MU (2018) Differences in leaf thermoregulation and water use strategies between three co-occurring Atlantic forest tree species: Leaf energy balance of Atlantic forest trees. Plant Cell Environ **41** : 1618–1631

Gasparini K, da Silva MF, Costa LC, Martins SCV, Ribeiro DM, Peres LEP, Zsogon A (2021) The Lanata trichome mutation increases stomatal conductance and reduces leaf temperature in tomato. Journal of Plant Physiology **260** : 153413

Gates DM (1968) Transpiration and Leaf Temperature. Annu Rev Plant Physiol **19** : 211–238

Gonzalez-Dugo V, Zarco-Tejada P, Berni JA, Suarez L, Goldhamer D, Fereres E (2012) Almond tree canopy temperature reveals intra-crown variability that is water stress-dependent. Agricultural and Forest Meteorology **154** : 156–165

Grace J, Wilson J (1976) The Boundary Layer over a*Populus* Leaf. J Exp Bot **27** : 231–241

Guha A, Han J, Cummings C, McLennan DA, Warren JM (2018) Differential ecophysiological responses and resilience to heat wave events in four co-occurring temperate tree species. Environ Res Lett**13** : 065008

Holmes MG, Keiller DR (2002) Effects of pubescence and waxes on the reflectance of leaves in the ultraviolet and photosynthetic wavebands: a comparison of a range of species: *Ultraviolet leaf reflectance* . Plant, Cell & Environment **25** : 85–93

Impens II (1966) Leaf wetness, diffusion resistances and transpiration rates of bean leaves (Phaseolus vulgaris L.) through comparison of wet and dry leaf temperatures. Oecol. Plant 1:

Impens II, Stewart DW, Allen LH, Lemon ER (1967) Diffusive Resistances at, and Transpiration Rates from Leaves in Situ Within the Vegetative Canopy of a Corn Crop. Plant Physiol **42** : 99–104

Jones HG (2014) Plants and microclimate: a quantitative approach to environmental plant physiology.

Karabourniotis G, Kotsabassidis D, Manetas Y (1995) Trichome density and its protective potential against ultraviolet-B radiation damage during leaf development. Canadian Journal of botany **73** : 376–383

Karabourniotis G, Papadopoulos K, Papamarkou M, Manetas Y(1992) Ultraviolet-B radiation absorbing capacity of leaf hairs. Physiol Plant **86** : 414–418

Kortekamp A, Zyprian E (1999) Leaf Hairs as a Basic Protective Barrier against Downy Mildew of Grape. J Phytopathol **147** : 453–459

Leigh A, Sevanto S, Close JD, Nicotra AB (2017) The influence of leaf size and shape on leaf thermal dynamics: does theory hold up under natural conditions? Plant, Cell & Environment **40** : 237–248

Levin DA (1973) The Role of Trichomes in Plant Defense. The Quarterly Review of Biology **48** : 3–15

Linacre ET (1972) Leaf temperatures, diffusion resistances, and transpiration. Agricultural Meteorology **10** : 365–382

Lopez A, Molina-Aiz FD, Valera DL, Pena A (2012) Determining the emissivity of the leaves of nine horticultural crops by means of infrared thermography. Scientia Horticulturae **137** : 49–58

Meerdink S, Roberts D, Hulley G, Gader P, Pisek J, Adamson K, King J, Hook SJ (2019) Plant species' spectral emissivity and temperature using the hyperspectral thermal emission spectrometer (HyTES) sensor. Remote Sensing of Environment **224** : 421–435

Meinzer F, Goldstein G (1985) Some consequences of leaf pubescence in the Andean giant rosette plant Espeletia timotensis. Ecology **66** : 512–520

Monteith JL, Unsworth MH (2013) Principles of environmental physics: plants, animals, and the atmosphere, 4. ed. Elsevier / Academic Press, Amsterdam Heidelberg

Nobel PS (1975) Effective Thickness and Resistance of the Air Boundary Layer Adjacent to Spherical Plant Parts. J Exp Bot **26** : 120–130

Nobel PS (2005) Physiochemical and Environmental Plant Physiology, 3rd ed. Elsevier Science & Technology

Ntefidou M, Manetas Y (1996) Optical Properties of Hairs During the Early Stages of Leaf Development in Platanus orientalis. Functional Plant Biol **23** : 535

Parkhurst DF (1976) EFFECTS OF VERBASCUM THAPSUS LEAF HAIRS ON HEAT AND MASS TRANSFER: A REASSESSMENT. New Phytol **76** : 453–457

Paw U KT, Daughtry CST (1984) A new method for the estimation of diffusive resistance of leaves. Agricultural and Forest Meteorology**33** : 141–155

Peng D-L, Niu Y, Song B, Chen J-G, Li Z-M, Yang Y, Sun H (2015) Woolly and overlapping leaves dampen temperature fluctuations in reproductive organ of an alpine Himalayan forb. Journal of Plant Ecology**8** : 159–165

Perez-Estrada LB, Cano-Santana Z, Oyama K (2000) Variation in leaf trichomes of Wigandia urens: environmental factors and physiological consequences. Tree Physiology **20** : 629–632

de Pury DGG, Farquhar GD (1997) Simple scaling of photosynthesis from leaves to canopies without the errors of big-leaf models. Plant, Cell and Environment **20** : 537–557

Raschke K (1960) Heat Transfer Between the Plant and the Environment. Annu Rev Plant Physiol **11** : 111–126

Richardson AD, Aubrecht DM, Basler D, Hufkens K, Muir CD, Hanssen L (2021) Developmental changes in the reflectance spectra of temperate deciduous tree leaves and implications for thermal emissivity and leaf temperature. New Phytol **229** : 791–804

Ripley BS, Pammenter N, Smith VR (1999) Function of leaf hairs revisited: the hair layer on leaves Arctotheca populifolia reduces photoinhibition, but leads to higher leaf temperatures caused by lower transpiration rates. Journal of Plant Physiology **155** : 78–85

Samarasekara SAL, Coorey RV (2011) Thermal capacity as a function of moisture content of Sri Lankan wood species: Wheatstone bridge method. Sri Lanka 9

Schlichting H, Gersten K (2017) Boundary-Layer theory, Ninth edition. Springer, Berlin Heidelberg

Schreuder MDJ, Brewer CA, Heine C (2001) Modelled Influences of Non-exchanging Trichomes on Leaf Boundary Layers and Gas Exchange. Journal of Theoretical Biology **210** : 23–32

Schuepp PH (1993) Tansley Review No. 59 Leaf boundary layers. New Phytol **125** : 477–507

Vialet-Chabrand S, Lawson T (2019) Dynamic leaf energy balance: deriving stomatal conductance from thermal imaging in a dynamic environment. Journal of Experimental Botany **70** : 2839–2855

Vogel S (1984) The lateral thermal conductivity of leaves. Can J Bot **62** : 741–744

Werker E (2000) Trichome diversity and development. Advances in Botanical Research. Elsevier, pp 1–35

Wolpert A (1962) Heat Transfer Analysis of Factors Affecting Plant Leaf Temperature. Significance of Leaf Hair. Plant Physiol**37** : 113–120

Woolley JT (1964) Water Relations of Soybean Leaf Hairs 1. Agronomy Journal **56** : 569–571

Wuenscher JE (1970a) THE EFFECT OF LEAF HAIRS OF VERBASCUM THAPSUS ON LEAF ENERGY EXCHANGE. New Phytol **69** : 65–73

Wuenscher JE (1970b) The effect of leaf hairs of Verbascum thapsus on leaf energy exchange. New Phytologist **69** : 65–73

Wullschleger SD (1993) Biochemical limitations to carbon assimilation in C3 plants–A retrospective analysis of the A/ci curves from 109 species. Journal of Experimental Botany **44** : 907–920

Xu X, Riley WJ, Koven CD, Jia G, Zhang X (2020) Earlier leaf-out warms air in the north. Nat Clim Chang **10** : 370–375

Zhang Y, Song H, Wang X, Zhou X, Zhang K, Chen X, Liu J, Han J, Wang A (2020) The Roles of Different Types of Trichomes in Tomato Resistance to Cold, Drought, Whiteflies, and Botrytis. Agronomy**10** : 411

Tables

Table 1 . Symbols used in the main text of this study.

description	symbol	units
composite parameter ($Q - 2\epsilon\sigma {T_\mathrm{a}}^4 - \lambda\gamma_\mathrm{tw} D_\mathrm{a}$)	a	J m^{-2} s^{-1}
composite parameter ($8\epsilon\sigma {T_\mathrm{a}}^3 + c_\mathrm{pa} g_\mathrm{bh} + \lambda\gamma_\mathrm{tw} s$)	b	J m^{-2} s^{-1} K^{-1}
ratio of adaxial to abaxial boundary layer resistance in abscence of hairs	β	-
heat capacity of air	c_pa	J mol^{-1} K^{-1}
difference between leaf and air temperature	δ	K
water vapor mole fraction deficit of the air	D_a	mol mol^{-1}
final value of δ	δ_f	K
depth of hair (trichome) layer	d_h	m
binary diffusivity for heat in air	D_ha	m^2 s^{-1}
initial value of δ	δ_i	L
leaf size (characteristic dimension)	d_l	m
leaf dry mass	DM	g
leaf to air water vapor mole fraction difference	Δw	mol mol^{-1}
leaf thermal emissivity	ϵ	-
boundary layer conductance to heat	g_bh	mol m^{-2} s^{-1}
leaf surface conductance to water vapor	g_sw	mol m^{-2} s^{-1}
leaf total conductance to water vapor	g_tw	mol m^{-2} s^{-1}
leaf heat capacity	k	J m^{-2} K^{-1}
latent heat of vaporization	λ	J mol^{-1}
leaf area	LA	m^2
absorbed radiation	Q	J m^{-2} s^{-1}
gas constant	R	Pa m^3 mol^{-1} K^{-1}
resistance added by hairs at one leaf surface	r_h	m^2 s mol^{-1}
derivative of w_s with respect to temperature	s	mol mol^{-1} K^{-1}
Stefan-Boltzmann constant	σ	J m^{-2} s^{-1} K^{-4}
leaf temperature	T	K

description	symbol	units
air temperature	T_a	K
wind speed	v_w	m s^{-1}
ambient water vapor mole fraction	w_a	mol mol^{-1}
leaf fresh mass	WM	g
saturated value of water vapor mole fraction	w_s	mol mol^{-1}
water use efficiency	WUE	mmol mol^{-1}
time constant for leaf cooling	τ	s

Table 2 . Species and genotypes examined in this study. Four-letter species codes are given in parentheses. *reps* : numbers of leaves, wind speeds, and cooling curves measured; *bald/hairy comparison* : whether measurements were compared between bald and hairy patches on the same leaf, or between bald and hairy leaves; *leaf heat capacity* : calculated from measured leaf area, water content and dry mass, assuming heat capacities of 4.184 and 1.5 J g^{-1} K^{-1} for water and dry mass, respectively. Trichome length (trichome layer depth) of the five experimental species. SOLY trichome depth was measured in 3-5 leaves for each species, except for SOLY, which was measured in images provided by Gasparini *et al.* (2021) for the same mutant (means ± SE).

species	reps	bald/hairy comparison	leaf heat capacity (J m^{-2} K^{-1})	μεαν τριχηομε δεπτη (μμ)
Olea europaea L.; Oleaceae (OLEU)	5 leaves x 4-5 curves	patches	1002 – 1140	135 ± 12
Magolia grandiflora L.; Magnoliaceae (MAGR)	5 leaves x 5 curves	patches	1107 – 1174	149 ± 3
Platanus occidentalis L.; Platanaceae (PLOC)	5 leaves x 3 curves	patches	507 – 1394	279 ± 23
Populus tomentosa L.; Salicaceae (POTO)	6 pairs of leaves x 3 curves	leaves	527 – 730	262 ± 18
Solanum lycopersicum, var. Ailsa Craig) mutants *Wo* (wooly) and *h* (hairless); Solanaceae (SOLY)	5 pairs of leaves x 3 curves	leaves	456 – 1192	780 ± 63

Table 3 . Leaf surface conductance to water vapor for the abaxial leaf surface in hairy and bald patches of leaves (OLEU, MAGR, PLOC) or hairy and bald leaves (POTO, SOLY), measured immediately before cooling curve experiments. Means ± SE; n=5 leaves except n=6 for POTO.

	leaf surface conductance to water vapor (mol m^{-2} s^{-1})	leaf surface conductance to water vapor (n
species	hairy	bald
OLEU	0.021 ± 0.004	0.022 ± 0.005

	leaf surface conductance to water vapor (mol m^{-2} s^{-1})	leaf surface conductance to water vapor (n
MAGR	0.004 ± 0.001	0.007 ± 0.002
PLOC	0.072 ± 0.005	0.043 ± 0.012
POTO	0.034 ± 0.005	0.070 ± 0.007
SOLY	0.026 ± 0.001	0.052 ± 0.006

Figures

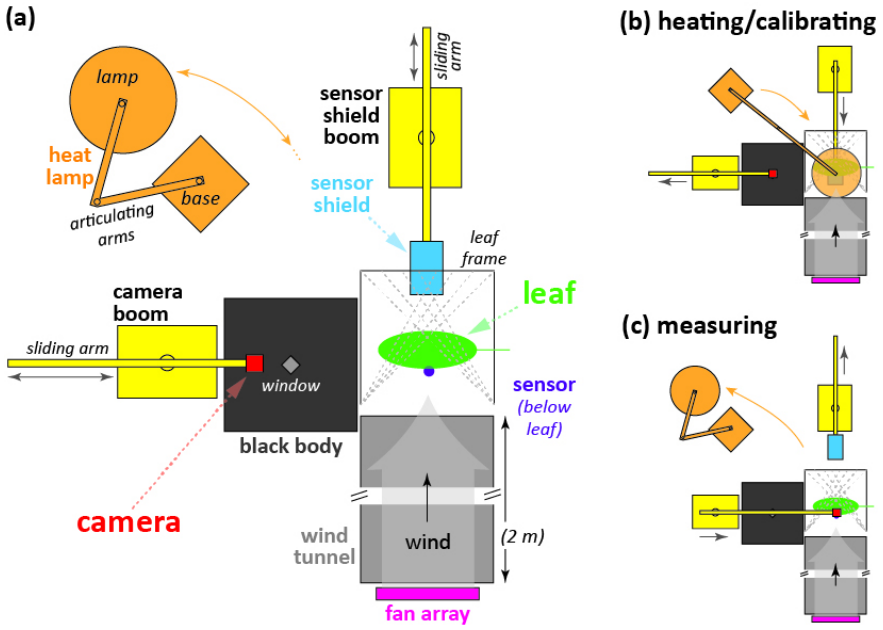

Figure 1 . Diagram of the system used to measure leaf boundary layer conductance in this study. (a) General layout. (b) Positions of components during heating of the leaf and calibration of the infrared camera: the camera is centered over the window into the black body, the air temperature/wind speed sensor shield is in place over the sensor, and the heat lamp is positioned over the leaf. (c) Positions of components during measurement of a cooling curve: the camera is positioned over the leaf, the heat lamp is rotated out of the way (positioned in the same plane as the leaf, and radiatively shielded using mylar-coated bubble wrap), and the sensor shield is moved back from below the leaf.

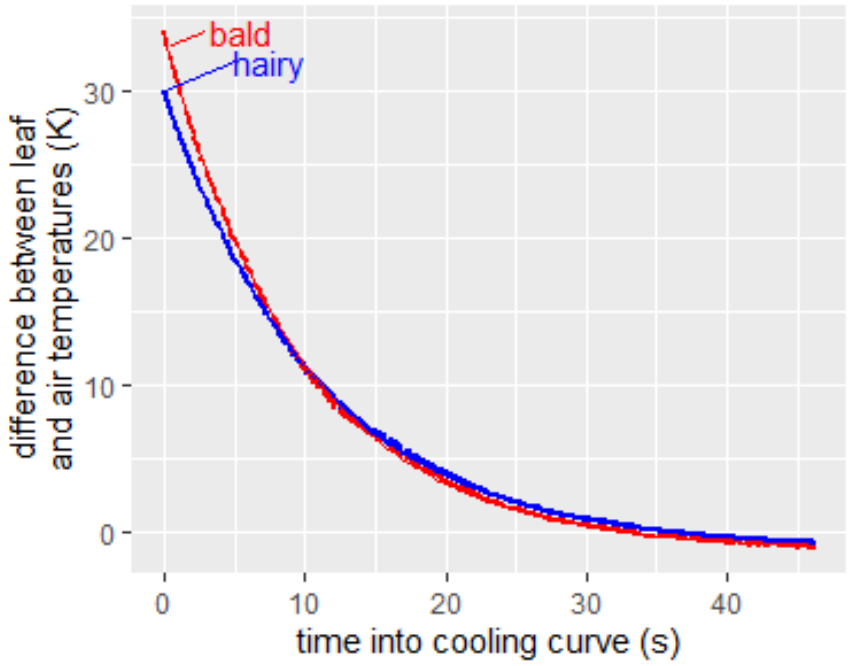

Figure 2 . Example of cooling curves for bald (red; hairs removed) and hairy (blue; hairs intact) patches adjacent to one another on the same OLEU leaf. Symbols = temperatures measured by infrared thermography; lines = model of leaf thermal dynamics fitted to the data. In this example, the time constants for cooling (τ) calculated from the fitted models were 9.79 and 10.94 seconds for the bald and hairy patches, respectively. Note: the symbols are plotted with a very small size so as not to obscure the close match between the fitted model and the data.

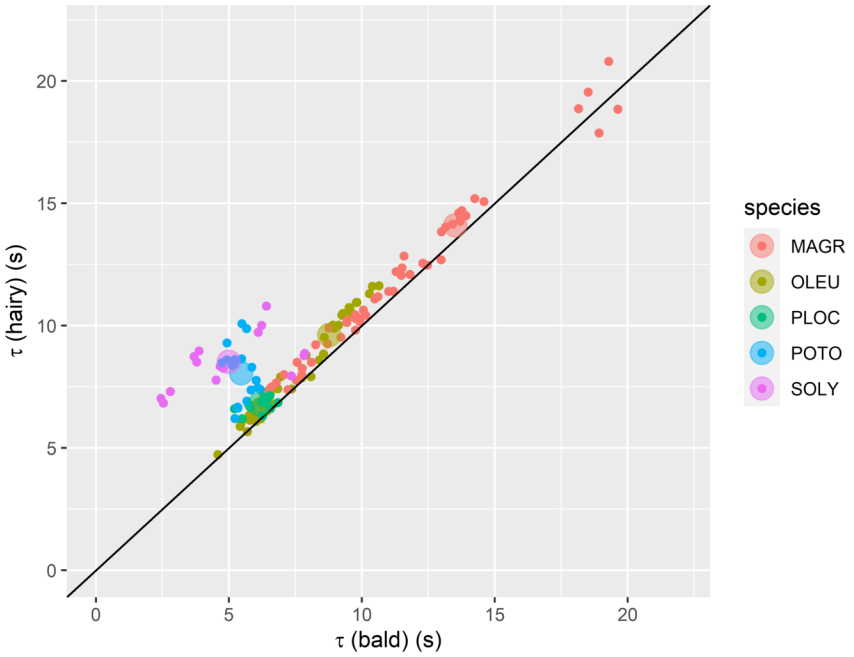

Figure 3 . Time constants for leaf cooling (τ) for bald vs. hairy patches on the same leaf (MAGR, OLEU and PLOC) or on different leaves (POTO, SOLY); in each case, the bald and hairy patches were at equal distances from the leading edge of the leaf and were measured simultaneously. Colors indicate species; small symbols represent results from individual cooling curves, and large semi-transparent symbols represent grand means within each species.

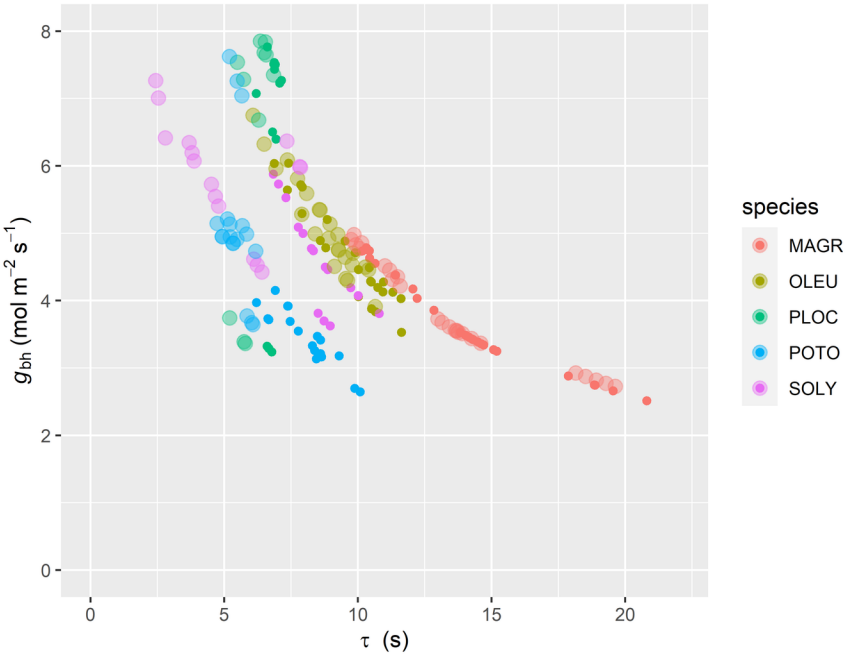

Figure 4 . Relationship between inferred boundary layer conductance to heat (g_{bh}) and time constant for leaf cooling (τ) for leaf patches. Colors indicate species; small, solid symbols denote hairy patches, and large, semitransparent symbols denote bald patches. Variation in the relationship of estimated g_{bh} to the measured τ within each species arises from differences in leaf heat capacity and stomatal conductance among leaves.

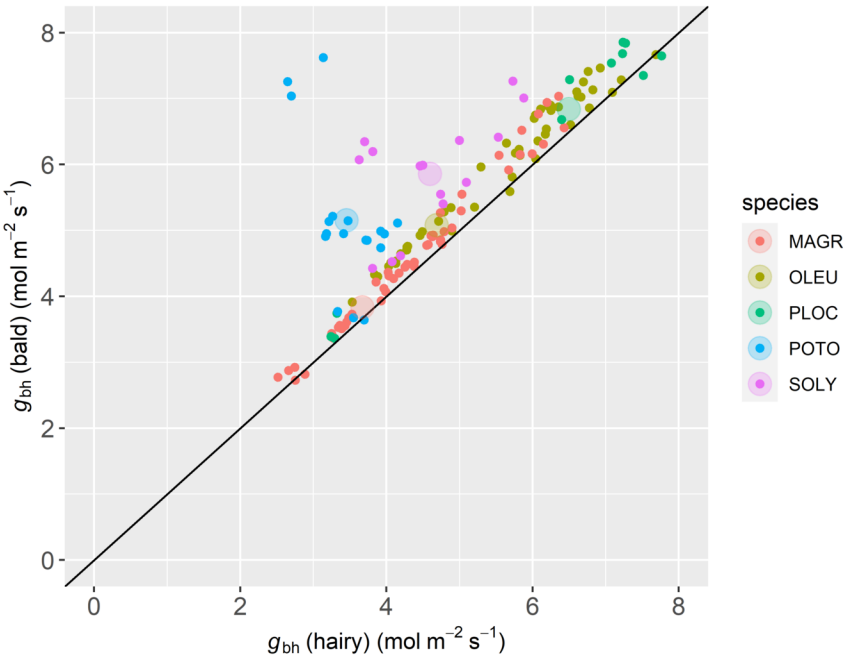

Figure 5 . Boundary layer conductance to heat (g_{bh}), inferred from time constants for leaf cooling, for bald vs. hairy patches on the same leaf (MAGR, OLEU and PLOC) or on different leaves (POTO, SOLY); in each case, the bald and hairy patches were at equal distances from the leading edge of the leaf and were measured simultaneously. Colors indicate species; small symbols represent results from individual cooling curves, and large semi-transparent symbols represent grand means within each species.

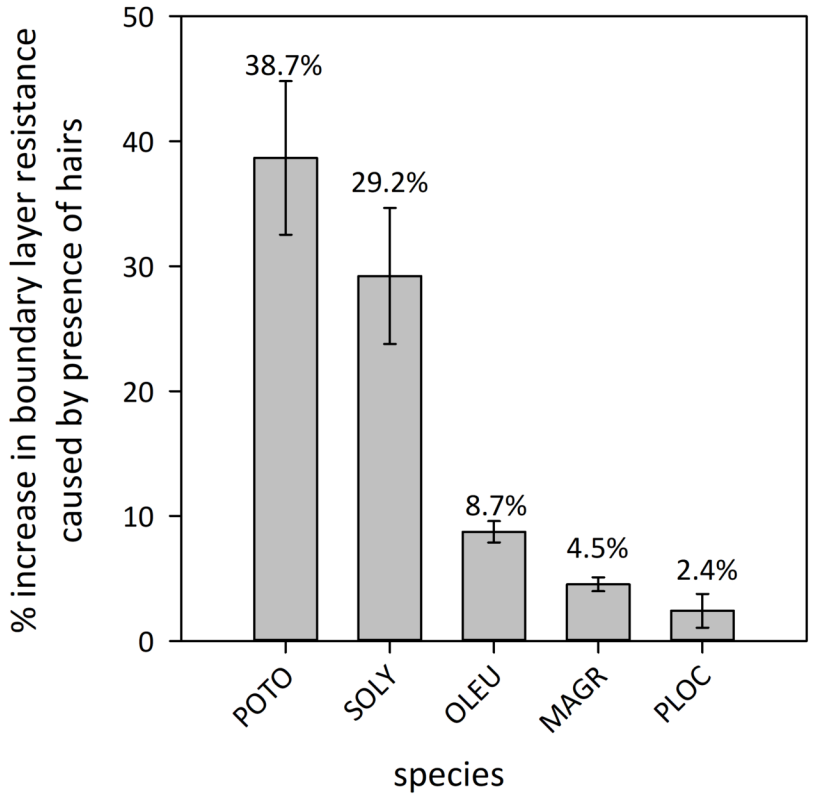

Figure 6 . Percent increase in whole-patch boundary layer resistance caused by the presence of hairs. Bars and values given above each bar are grand means within species; error bars are standard errors of the mean. Results presented here excluded one outlier leaf of POTO (corresponding to the largest values of g_{bh} in bald leaves of that species in Fig 5).

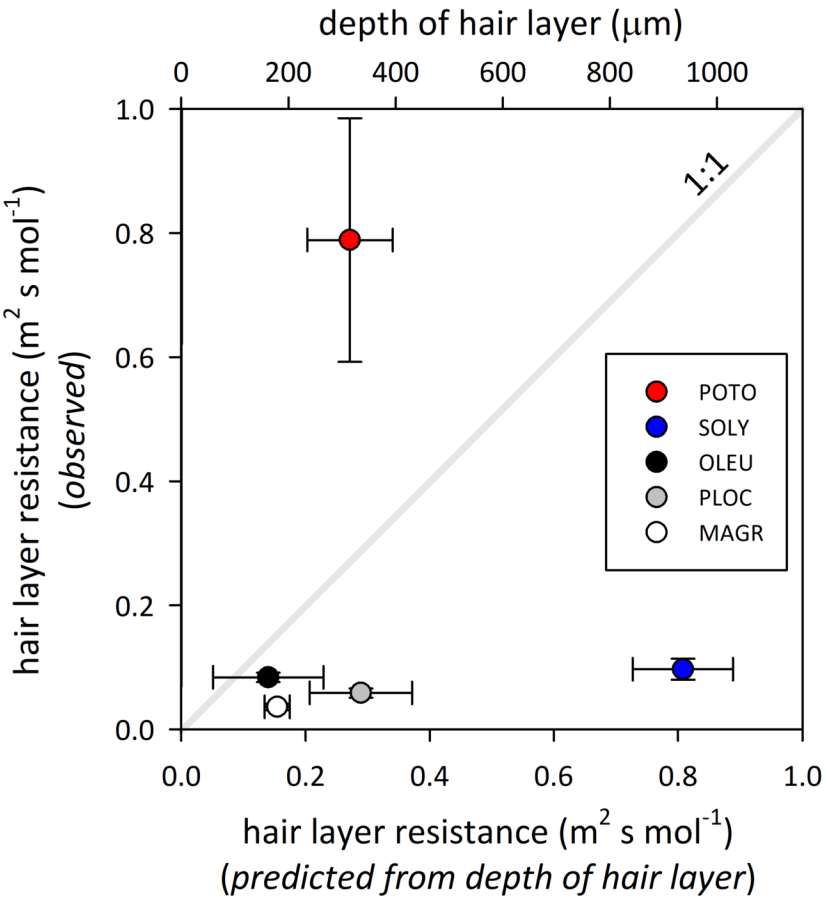

Figure 7 . The mean diffusive resistance added by hairs to one leaf surface, calculated from observed differences in boundary layer conductance between hairy and bald patches (vertical axis), was unrelated to theoretical predictions based on the thickness of the hair layer (horizontal axis) (regression n.s. [p = 0.90]). Theoretical predictions assumed hairs entrain a layer of perfectly still air, and did not attempt to account for the density of hairs or the tortuosity of diffusion pathways through the hair layer. The grey line represents the 1:1 relationship.

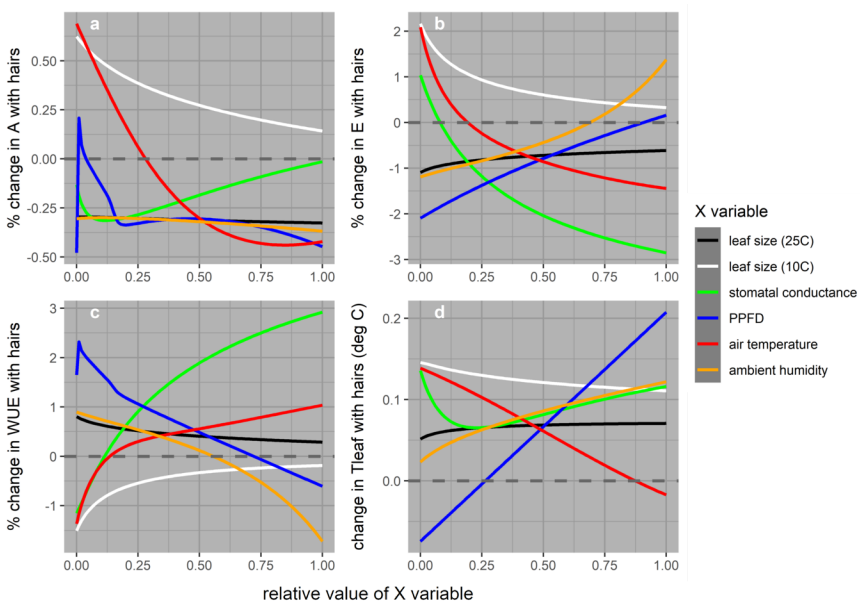

Figure 8 . Simulated effects of leaf hairs (contributing a resistance of $r_{\mathrm{h}} = 0.1$ m^2 s mol^{-1} on (a) net CO_2 assimilation rate (A), (b) transpiration rate (E), (c) water use efficiency (WUE = A/E), and (d) leaf temperature (T_{leaf}), under various conditions for the X variables listed in the legend. The ranges and default values for each X variable were as follows: leaf size (0.01 to 0.30 m, default 0.1), stomatal conductance (0.001 to 1.0 mol m^{-2}s^{-1}, default 0.18), PPFD (0 to 2000 μmol m^{-2} s^{-1}, default 1000), air temperature (5 to 45°C, default 25), and ambient humidity (0.002 to 0.03 mol mol^{-1}, default 0.01). Results for X = leaf size are shown for two air temperatures (25°C and 10°C). The dashed grey line indicates zero change. Note that % changes are shown for A ,E and WUE, whereas absolute changes are shown for T_{leaf}.